Available online at www.sciencedirect.com
ScienceDirect
Applied Catalysis B: Environmental 80 (2008) 15–23
APPLIED CATALYSIS B: ENVIRONMENTAL
www.elsevier.com/locate/apcatb

Review

Catalytic stability of Ni_3Al powder for methane steam reforming

Yan Ma [a,b,*], Ya Xu [a], Masahiko Demura [a], Toshiyuki Hirano [a,b]

[a] National Institute for Materials Science, 1-2-1 Sengen, Tsukuba, Ibaraki 305-0047, Japan
[b] Graduate School of Pure and Applied Sciences, University of Tsukuba, 1-2-1 Sengen, Tsukuba, Ibaraki 305-0047, Japan

Received 19 September 2007; received in revised form 16 October 2007; accepted 23 October 2007
Available online 7 November 2007

Abstract

We previously found catalytic activity for methane steam reforming in atomized Ni_3Al powder which was pretreated by acid and subsequent alkali leaching. In this study the catalytic stability of the pretreated Ni_3Al powder was investigated by isothermal test in the temperature range of 873–1173 K for 10 h. The activity was relatively stable over time at low temperatures below 973 K, especially at 873 K, where it retained the initial activity even after 10 h. However, it rapidly decreased with time at temperatures above 1073 K. Fine Ni particles, which were produced on the outer surface of Ni_3Al powder during the pretreatment and served as a catalyst, survived on the surface after tests at all the temperatures. They remained almost unchanged below 973 K, leading to the good stability, while sintering and oxidation occurred at high temperatures, leading to the rapid deactivation.

Keywords: Hydrogen production; Ni_3Al; Stability; Methane steam reforming

Contents

1. Introduction

Hydrogen is attracting high attention as a clean and efficient energy source. At present, most of the world's hydrogen is produced from natural gas (mainly methane) by a process called steam reforming [1–2]. Methane steam reforming (MSR) is an endothermic and catalyzed reaction of methane with excess steam to produce H_2 and CO/CO_2 [3–6]. Because Ni is

* Corresponding author at: Graduate School of Pure and Applied Sciences, 1-2-1 Sengen, Tsukuba, Ibaraki 305-0047, Japan. Tel.: +81 29 859 2511; fax: +81 29 859 2501.
E-mail address: MA.Yan@nims.go.jp (Y. Ma).

0926-3373/$ – see front matter © 2007 Elsevier B.V. All rights reserved.
doi:10.1016/j.apcatb.2007.10.034

economical and an active element [7–9], Ni catalysts, supported on ceramics, are industrially used in this process [10–12]. However, they are often subject to several types of deactivations, for example, sintering, oxidation, carbon deposition and sulfur poisoning [13]. It is necessary to develop more deactivation resistant catalysts.

Until now, intermetallic compound Ni_3Al is known as a promising high temperature material because of its excellent high temperature strength and good corrosion/oxidation resistance [14,15]. So far, no promising catalytic properties have been reported for this compound. However, recently our group found that Ni_3Al, in the form of both powder and foil exhibits high catalytic activity for methanol decomposition, leading to hydrogen generation ($CH_3OH \rightarrow 2H_2 + CO$) [16–19]. Inspired by these findings, we for the first time investigated the catalytic activity of Ni_3Al for MSR using atomized Ni_3Al powder [20]. It was found from the isochronal tests that the activity was significantly enhanced by a combined pretreatment of acid and subsequent alkali leaching, although its activity was quite low in the as-received or as-atomized state. The drastic enhancement was attributed to the formation of fine Ni particles on the porous surface of the pretreated Ni_3Al powder, as shown in the TEM analysis in Fig. 1 [20]. The results demonstrate the possibility of atomized Ni_3Al powder as a catalyst precursor for MSR.

In the present study, we investigated the stability of this new catalyst by isothermal tests. The chemical composition and the structure of the powder surface after test were characterized in order to determine the factors influencing the stability.

2. Experimental

2.1. Catalyst preparation

Catalyst samples were prepared in the same way as we previously reported [20]. A stoichiometric Ni_3Al (Ni-25 at.% Al) powder was obtained from Kojundo Chemical Lab. Co., Ltd., Japan. It was prepared by a gas atomizing process and sieved to less than 150 μm in size. Because it was rapidly solidified during the atomizing process, it had a second lamellar phase in the Ni_3Al matrix which was identified as $L1_0$-type β′-NiAl in our previous study [20]. The powder was pretreated in two steps, acid leaching and subsequent alkali leaching, which was found the most effective in enhancing the activity as described in our previous report [20]. At first, the powder was dipped in 2 vol.% aqueous HNO_3 at 298 K for 15 min (acid leaching), then rinsed in deionized water and dried at 323 K for 8 h. This first process preferentially dissolved the lamellar β′-NiAl from the surface of the powder, resulting in the formation of the porous surface. Next, the powder was dipped in a stirred 20 wt.% aqueous NaOH solution at 366 K for 300 min (alkali leaching), then rinsed in deionized water and dried at 323 K for 8 h. This process selectively leached Al from the Ni_3Al only in the outer surface, forming the fine Ni particles on the surface as shown in Fig. 1.

2.2. Catalytic reaction

Catalytic experiments were carried out in a conventional fixed-bed flow reactor at ambient pressure in the same way as described in the previous report [20]. A 0.4 g sample of the pretreated Ni_3Al powder was placed in a quartz tube with an internal diameter of 8 mm and the set into the stove of the reactor. The height of the powder was about 2 mm. Prior to the reaction, the powder was reduced at 873 K for 1 h in a flowing hydrogen atmosphere. The hydrogen flow was then stopped and filled with pure nitrogen to flush out the hydrogen. Temperature-programmed reduction (TPR) experiments confirmed that most of the NiO on the pretreated powder surface was reduced according to the previously reported literature [21–23], as shown in Fig. 2. The temperature was then increased to the given temperatures 873, 973, 1073, and 1173 K and kept constant at these temperatures. After 0.5 h waiting for the temperature to stabilize, the reactant mixture of CH_4 and H_2O stream (mole ratio of $H_2O/CH_4 = 3$) was introduced into the quartz tube with nitrogen carrier gas (mole ratio of $N_2/CH_4 = 1.5$) at a gas hourly space velocity of 12000 h^{-1} (defined as the volume of CH_4 passed over a unit volume of catalyst per

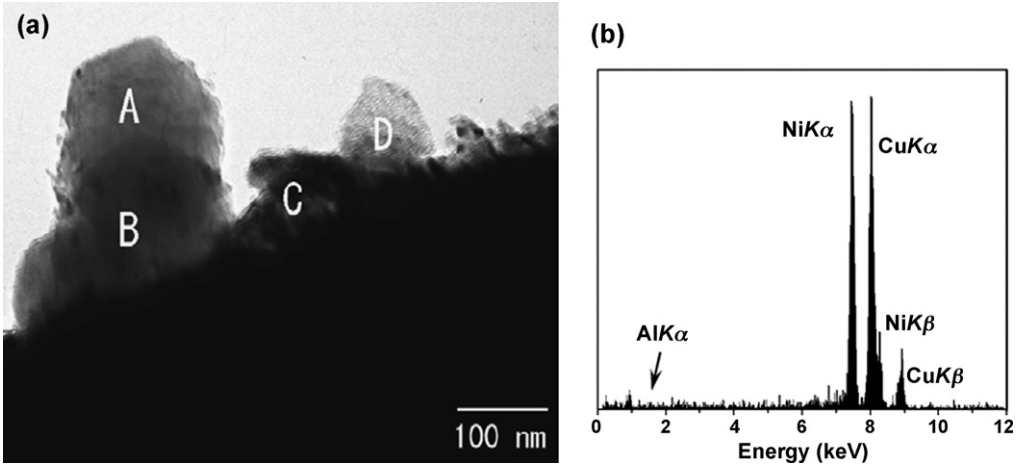

Fig. 1. (a) TEM bright field image of atomized Ni_3Al powder pretreated by acid and alkali leaching, showing the formation of fine Ni particles on the porous surface, and (b) EDS spectra taken from the surface showing that the particles are composed of pure Ni [20].

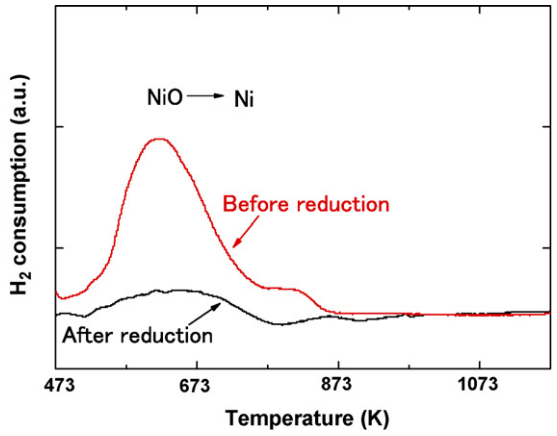

Fig. 2. TPR profiles of the pretreated Ni_3Al powder before and after reduction at 873 K for 1 h in a flowing hydrogen atmosphere.

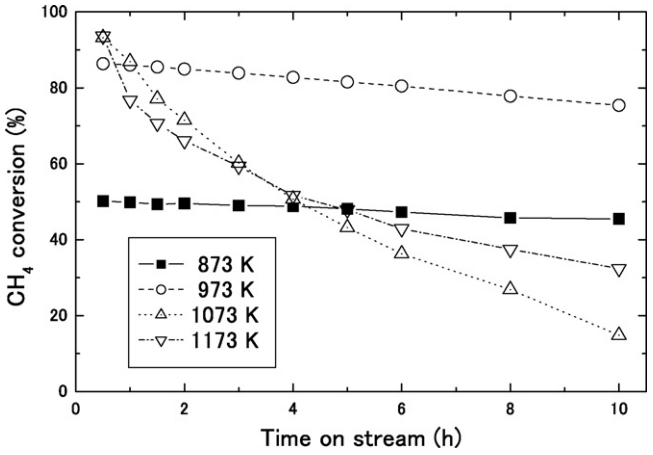

Fig. 3. CH_4 conversion during MSR over the pretreated Ni_3Al powder at 873, 973, 1073, and 1173 K as a function of reaction time.

hour). The H_2O was fully evaporated in a thermal evaporator before introducing into the reactor. The composition of the outlet gas products was analyzed using gas chromatographs (GL Science, GC-323 equipped with thermal conductivity detectors). The total flow rate of the gas products was measured using a soap bubble meter just after the gas analysis.

2.3. Surface characterization

Before and after the isothermal tests, the surface area of the powders was determined by the Brunauer–Emmett–Teller (BET) surface area analysis method using krypton adsorption (Micromeritics, ASAP 2020). Surface products were formed on the powder during the isothermal tests. Their crystal structures were analyzed by X-ray diffraction (XRD) using a Cu Kα source (Rigaku, RINT2500). Their morphologies were observed on the surface and the cross section of the powder by scanning electron microscopy (SEM: JEOL, JSM-7000F). The surface structure and composition were determined by transmission electron microscopy (TEM: Hitachi, 2000HF-FE) coupled with an X-ray energy dispersive spectroscopy (EDS) system. The TEM samples were prepared, as follows: the powder was dispersed in ethanol by ultrasonic agitation, and then the suspension was dropped on a TEM Cu grid with a carbon mesh film and finally dried in air.

3. Results

3.1. Catalytic behavior

The catalytic performances of the pretreated Ni_3Al powder for MSR were investigated at temperatures of 873, 973, 1073, and 1173 K for 10 h. The CH_4 conversion is plotted as a function of reaction time, as shown in Fig. 3. We define the value after the first 0.5 h reaction as the ''initial conversion''. As we previously reported in the isochronal tests [20], the initial conversion rapidly increases with temperature and reaches a maximum of 95% at 1073 K. The variation in the CH_4 conversion with time strongly depends on the reaction temperature. At 873 K, the conversion remains stable over time, showing no considerable change after 10 h, although it is relatively low, about 50%. At 973 K, the conversion slightly decreases from 86 to 76% after 10 h. In contrast, the conversion decreases rapidly at and above1073 K: it decreases from 95 to 30% at 1073 K and to 18% at 1173 K. Thus, it turned out that the stability of the pretreated Ni_3Al powder is good below 973 K but becomes poor above that.

Three gaseous products, H_2, CO and CO_2, were detected at the outlet of the reactor by gas chromatography. The amount of carbon atoms maintained a balance within a maximum of 3%. Fig. 4 shows the gas production rates at four reaction temperatures as a function of reaction time. We calculated the production rate R_i of gaseous species i using the following equation:

$$R_i = \frac{C_i \times F_{\text{Total}}}{W}$$

where C_i and F_{Total} are the volume fraction of i in total outlet gases and the flow rate of total outlet gases (ml min^{-1}) excluding H_2O, respectively, and W is the weight of the pretreated Ni_3Al powder (g).

As shown in Fig. 4, the initial production rates of H_2 and CO monotonously increase with increasing temperature up to1073 K and then tend to become saturated in the same way as the initial CH_4 conversion. The initial production rate of CO_2 behaves differently from those of H_2 and CO as we previously reported in the isochronal tests [20]. It increases with increasing temperature up to 1073 K but conversely decreases above 1073 K.

All the production rates show the same time dependence as the CH_4 conversion. They are rather stable over time below 973 K. They remain constant at 873 K and slightly decrease with time at 973 K. At and above 1073 K, they decrease rapidly with time. In detail, the production rate of CO_2 decreases slowly compared to those of the H_2 and CO production rates, suggesting that the production of CO_2 is less sensitive to temperature.

3.2. Surface characterization

The BET surface areas of the pretreated powder before and after 10-h reaction are listed in Table 1. In our previous study

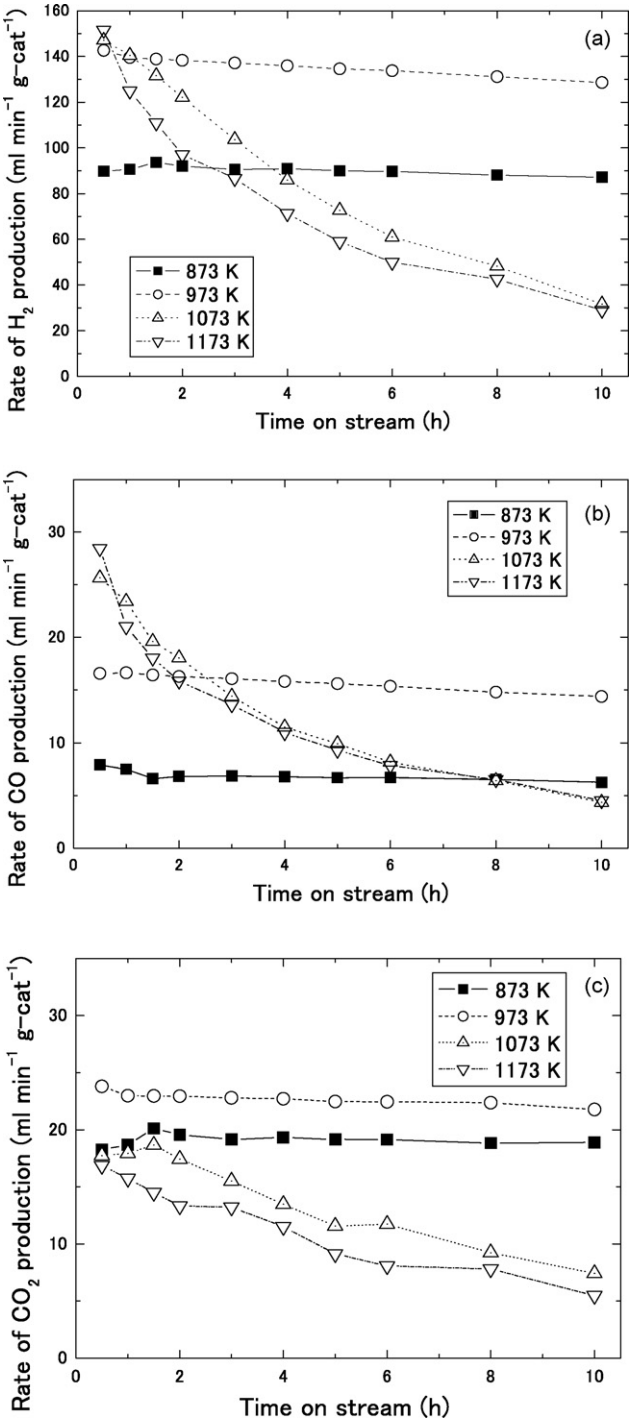

Fig. 4. Production rates of (a) H_2, (b) CO, and (c) CO_2 during MSR over the pretreated Ni_3Al powders at 873, 973, 1073, and 1173 K as a function of reaction time.

[20], we reported that fine Ni particles were formed on the powder surface by the pretreatment, leading to the increase in surface area from 0.06 m^2/g of the as-received state to 0.41 m^2/g. The surface area slightly decreased after reaction at 873 K and decreased by 65% after reaction at 973 K. At higher temperature above 1073 K, the surface area decreased significantly to approximately one quarter.

The structures of the powder after 10-h reaction were examined by XRD, as shown in Fig. 5. Fine Ni particles shown in Fig. 1 are present on the powder before reaction, but they are not detected in the XRD pattern because they are very fine and exist only as a very thin layer on the outer surface. No change is observed in the XRD pattern after the reaction at 873 K. With increasing temperature, the metallic Ni phase becomes detectable above 973 K, implying that the fine Ni particles agglomerated. In addition to the Ni phase, NiO and Al_2O_3 phases are identified after the reaction at 1073 K and 1173 K, respectively. The pretreated Ni_3Al powder was found to be partly oxidized at higher temperatures.

Table 1
BET surface areas of the pretreated Ni_3Al powders before and after 10-h reaction

Before reaction (m^2/g)	After 10-h reaction (m^2/g)			
	873 K	973 K	1073 K	1173 K
0.41	0.39	0.27	0.12	0.10

The SEM morphologies of the powder surface after the 10-h test at different temperatures are shown in Fig. 6. For comparison, the surface morphology before reaction is also shown in the figure (Fig. 6(a)). The surface is rough and porous before reaction. It consists to some extent of an aligned columnar structure which is a skeleton produced by the preferential dissolution of lamellar β′-NiAl in the first step of the pretreatment. The fine Ni particles shown in Fig. 1 exist on the surface of the columnar structure, though they are not visible in the SEM observation. There we observed a change in the morphology of the columnar structure after the isothermal tests at all the reaction temperatures, as shown in Fig. 6(b)–(e). The columnar structure changes into particles, having crystal faces. The particle size becomes larger with increasing temperature. Another characteristic feature is that carbon deposition is hardly observed at all the temperatures.

SEM observation was also performed on the cross sections of the Ni_3Al powder after a 10-h test using the backscattering electron mode and EDS analysis. Fig. 7(a)–(d) show that a layer

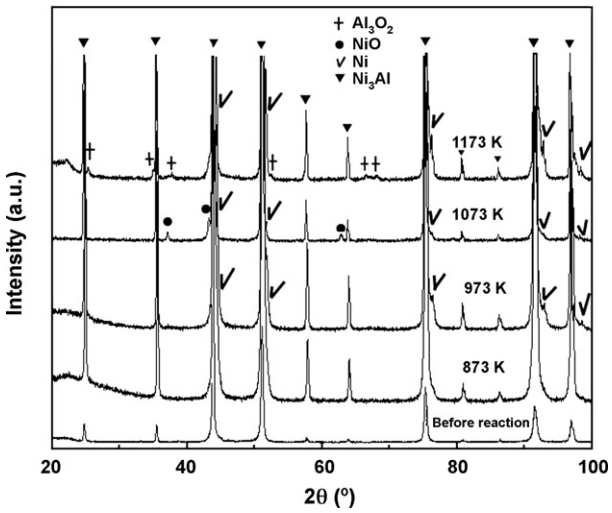

Fig. 5. XRD patterns of the pretreated Ni_3Al powders (a) before reaction and after 10-h reaction at (b) 873 K, (c) 973 K, (d) 1073 K, and (e) 1173 K.

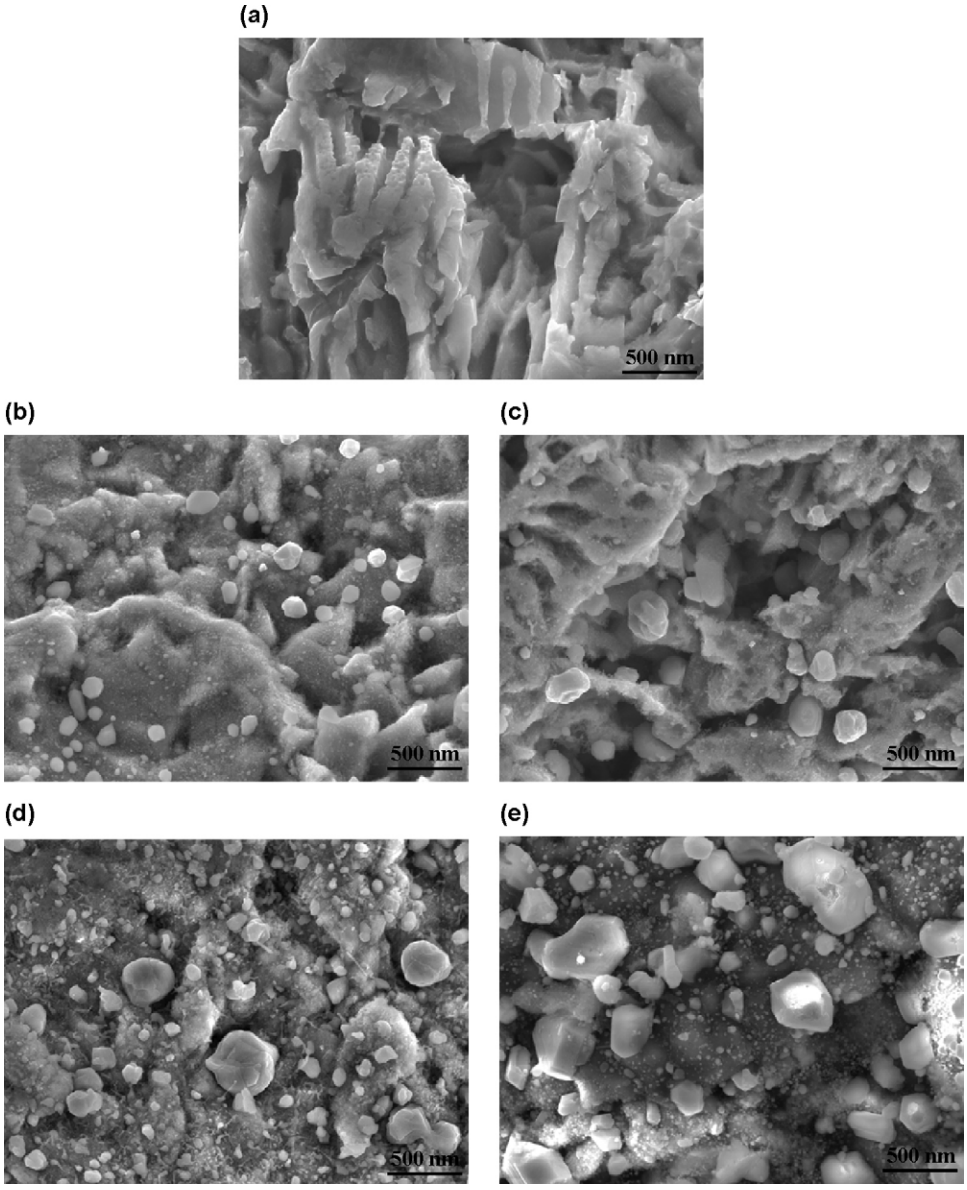

Fig. 6. SEM images of the pretreated Ni_3Al powder (a) before reaction and after 10-h reaction at (b) 873 K, (c) 973 K, (d) 1073 K, and (e) 1173 K, showing the surface morphology change.

product with a grey contrast is formed on the rough surface corresponding to the columnar structure. The grey layer is very thin after the reaction at 873 K and becomes thicker with increasing temperature. In addition, many small particles with bright contrast are dispersed on and within the grey layer. They also grow larger with the increasing temperature. EDS analysis was performed on the one of the large particles after the reaction at 1073 K (shown by a circle in Fig. 7(c)). Fig. 7(e) shows that the particles are highly concentrated in Ni. This indicates that the fine Ni particles, which were produced in the pretreatment, agglomerated into large ones during the reaction, and thus they were detectable in the XRD pattern (Fig. 5). EDS analysis was also performed on the grey layer after the reaction at 1173 K (shown by an arrow in Fig. 7(d)). Fig. 7(f) shows that the grey layer is enriched in O, Al and Ni. It is clear that the surface of the Ni_3Al powder is oxidized during the reaction at the higher temperature, which is consistent with the results of XRD (Fig. 5).

The surface structure of the powder after 10-h reaction was examined using TEM coupled with EDS. Fig. 8(a) shows the bright field image of the surface after the reaction at 873 K. The surface is mostly covered by particles with a crystal face. The EDS spectra in Fig. 8(b) show that the particles are Ni, indicating that the fine Ni particles which were produced in the pretreatment remain on the surface after the reaction. The existence of Ni particles was similarly observed after the reaction at 973 K. In addition, it was found that the Ni particles were partly oxidized to form NiO by the EDS spectra and the selected area diffraction pattern at 973 K (not shown here). The surface structure changed more obviously above 1073 K. Fig. 9 shows the TEM analysis after the reaction at 1073 K. Al_2O_3 is observed (position C) in addition to Ni (position A) and NiO (position B), which is consistent with the results of the cross-sectional SEM analysis (Fig. 7). After the reaction at 1173 K, another oxide

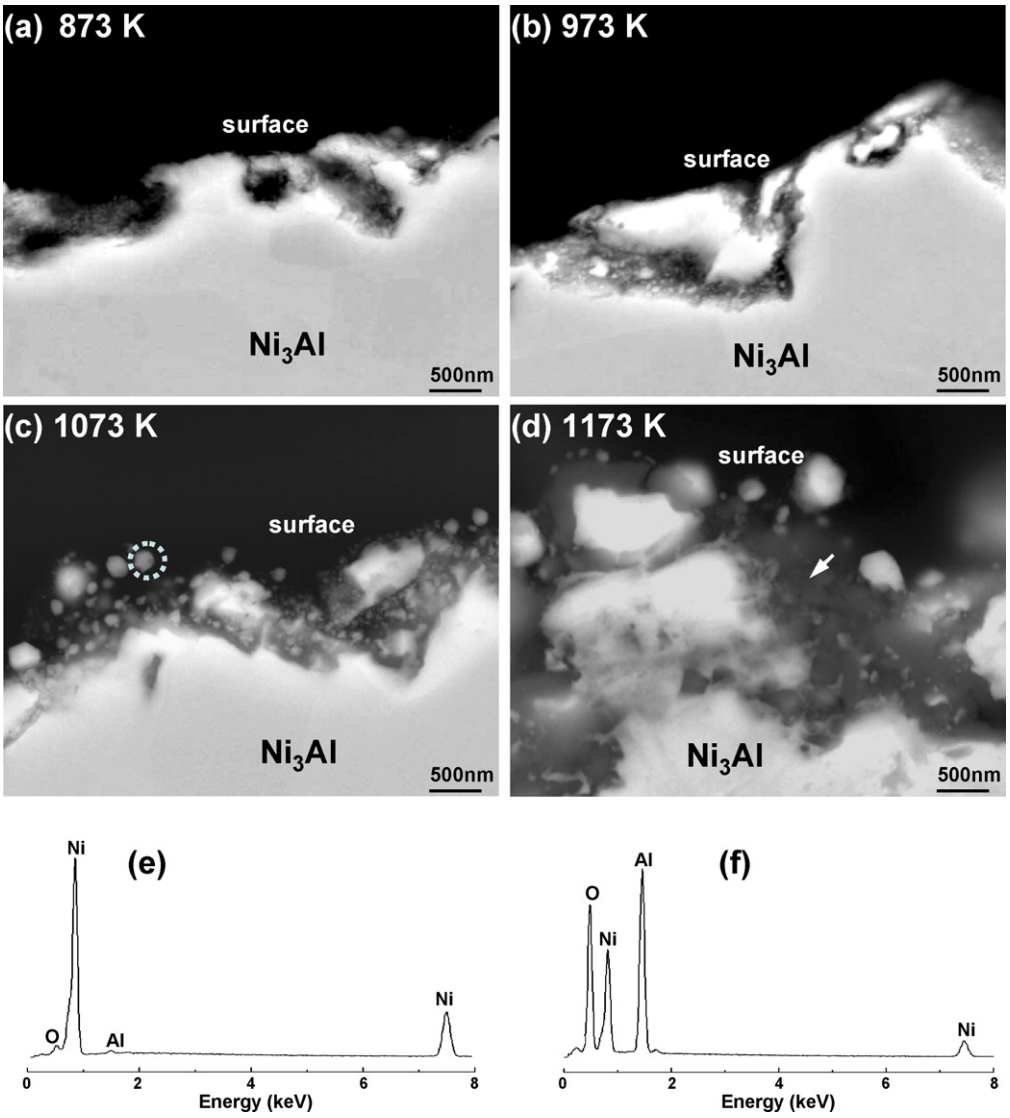

Fig. 7. Backscattered electron images of the cross section of the pretreated Ni_3Al powders after 10-h reaction at (a) 873 K, (b) 973 K, (c) 1073 K, and (d) 1173 K. EDS spectra taken from (e) the particles indicated by the arrow in (c) and (f) the grey regions indicated by the arrow in (d).

containing Al and a small amount of Ni is observed as shown in Fig. 10, in addition to Ni, NiO and Al_2O_3. This oxide was identified as $NiAl_{10}O_{16}$ by the selected area diffraction pattern (not shown here).

The surface structures of the powder which were identified by XRD, SEM and TEM are summarized in Table 2. It is noted that the fine Ni particles which were produced in the pretreatment remained at all the temperatures. Ni was partly oxidized to form NiO above 973 K. Al was oxidized to form Al_2O_3 above 1073 K and partly to form the complicated oxide $NiAl_{10}O_{16}$ at 1173 K.

4. Discussion

4.1. Catalytic reaction

In this study, isothermal tests were performed to examine the stability of the catalytic performance of the pretreated Ni_3Al powder for MSR in the temperature range of 873–1173 K. As shown in Fig. 3, the activity of the powder was found to be stable over time below 973 K and to decrease rapidly with time above 973 K. We will discuss the characteristic features of the catalytic reaction over the pretreated Ni_3Al powder.

As we previously reported [20], the following two reversible chemical reactions can be assumed for the MSR over the pretreated Ni_3Al powder under excess steam ($H_2O/CH_4 = 3$) conditions:

$$CH_4 + H_2O \Leftrightarrow 3H_2 + CO \quad \Delta H^0_{298} = +206\,\mathrm{KJ/mol} \tag{1}$$

$$CO + H_2O \Leftrightarrow H_2 + CO_2 \quad \Delta H^0_{298} = -41\,\mathrm{KJ/mol} \tag{2}$$

This assumption is valid through the entire reaction because carbon maintained a balance between the inlet and outlet carbon-containing gases, and the molecule numbers of H_2, CO and CO_2 held to be a stoichiometric relation in Eqs. (1) and (2).

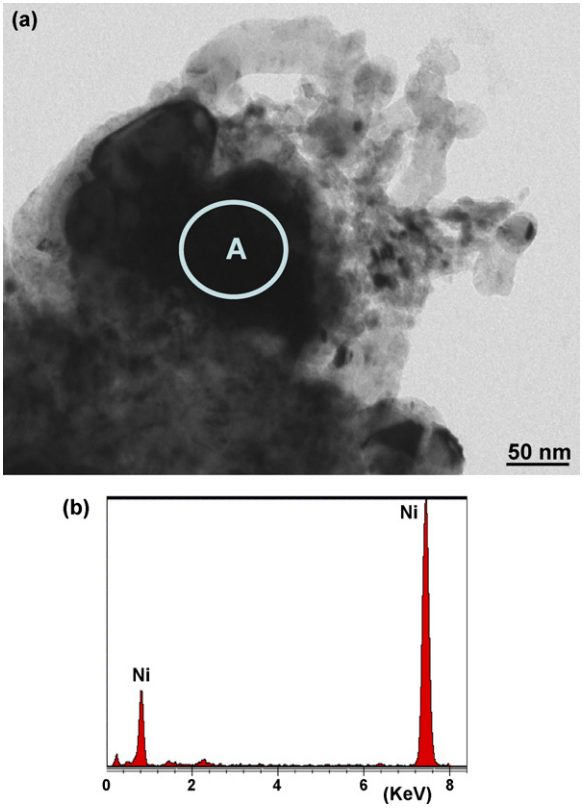

Fig. 8. (a) TEM bright field image of the powder surface after reaction at 873 K. (b) EDS spectra taken from position A, showing the presence of fine Ni particles.

Thus, the selectivities of CO (S_{CO}) and CO_2 (S_{CO_2}) can be calculated from the production rates of the products as:

$$S_{CO}\,(\%) = \frac{R_{CO}}{R_{inletCH_4} - R_{ouletCH_4}} \times 100 \quad (3)$$

$$S_{CO_2}\,(\%) = \frac{R_{CO_2}}{R_{inletCH_4} - R_{ouletCH_4}} \times 100 \quad (4)$$

where $R_{inletCH_4}$ and $R_{outletCH_4}$ are the inlet and outlet flow rates of CH_4 per unit weight of catalyst, respectively. Fig. 11 shows the selectivities of CO and CO_2 as a function of reaction time at the four temperatures.

At the initial time of reaction, the selectivities of CO and CO_2 show positive and negative temperature dependences, respectively. As we discussed in the previous study [20], this is consistent with the endothermic character of MSR and the exothermic character of WGS.

Both the selectivities remained stable during the reaction below 973 K. Remembering that the CH_4 conversion also remained stable in this temperature range (Fig. 3), the stable selectivity means that both the MSR and WGS are stably catalyzed over the pretreated Ni_3Al powder. On the other hand, the selectivity of CO decreased rapidly with time and that of CO_2 slowly increased above 1073 K. The decrease in CO selectivity must be due to the loss of activation for the MSR due to the decrease in the CH_4 conversion with time (Fig. 3). The behavior of CO_2 selectivity, however, may seem strange,

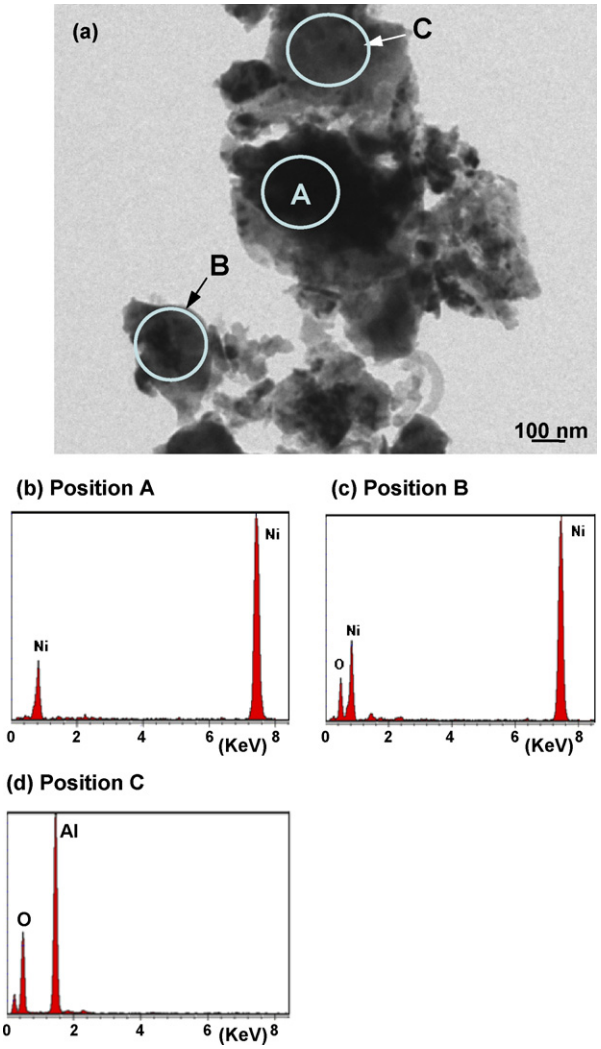

Fig. 9. (a) TEM bright field image of the surface after reaction at 1073 K, (b) EDS spectra taken from position A, showing the presence of fine Ni particles, (c) EDS spectra taken from position B, showing the formation of NiO, (d) EDS spectra taken from position C, showing the formation of Al_2O_3.

considering the decrease in the production rate of CO_2 with time. This is probably because the production rate of CO_2 decreased more slowly than those of H_2 and CO as shown in Fig. 4(c), i.e., the production rate of CO_2 decreased more slowly than the CH_4 conversion. It is likely that the catalytic activity of the pretreated Ni_3Al powder is not stable for the MSR but rather stable for the WGS even above 1073 K.

4.2. Stability and deactivation

As we previously reported [20], fine Ni particles (Fig. 1) were dispersed on the porous surface (Fig. 6(a)) in the pretreatment of atomized Ni_3Al powder. Both the fine Ni particles and the porous surface must be essential for the activity for MSR, i.e., the fine Ni particles serve as a catalyst and the porous surface as a support. We will discuss the stability of the catalytic activity of the pretreated Ni_3Al powder based on the characterization of the surface structure.

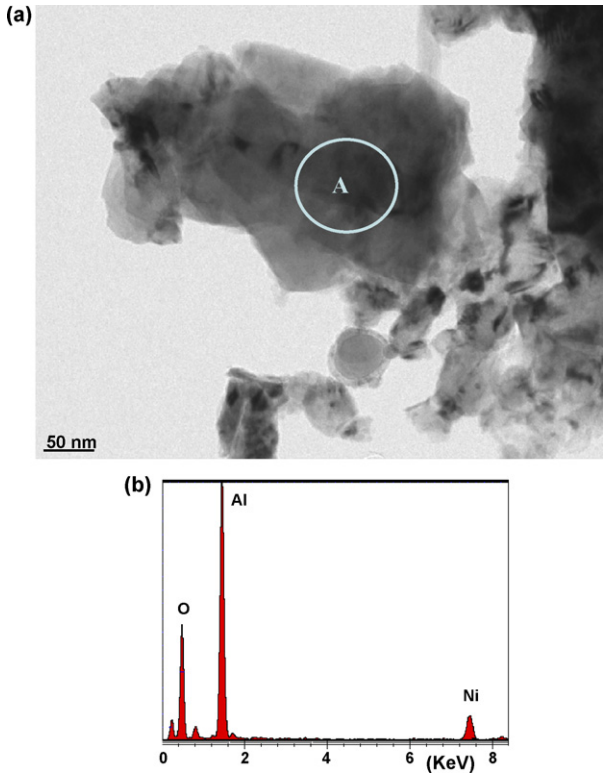

Fig. 10. (a) TEM bright field image of the surface after reaction at 1173 K, (b) EDS spectra taken from position A, showing the formation of $NiAl_{10}O_{16}$.

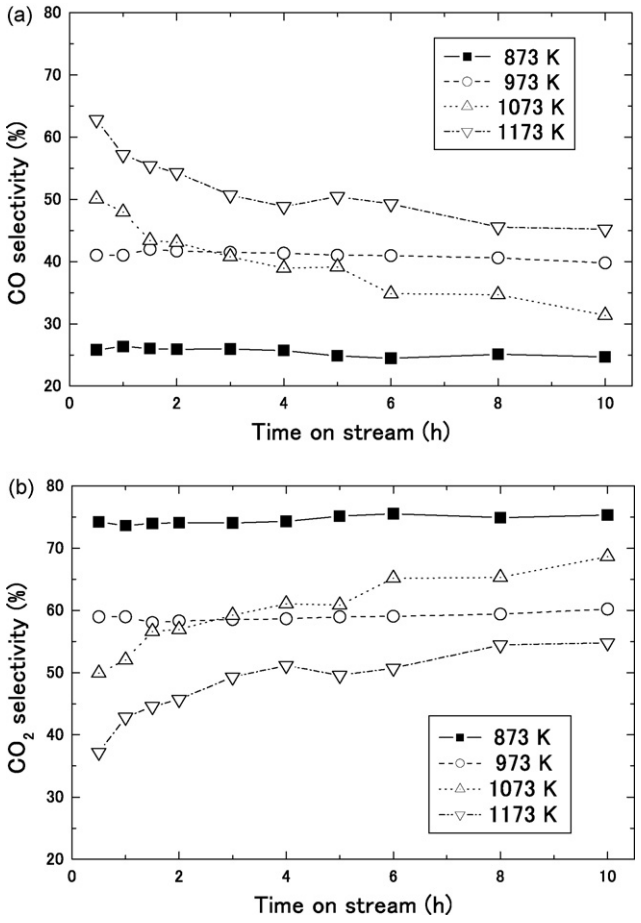

Fig. 11. (a) CO and (b) CO_2 selectivities during MSR over the pretreated Ni_3Al powder at 873, 973, 1073, and 1173 K as a function of reaction time.

The fine Ni particles remained on the surface after the reaction at all reaction temperatures as summarized in Table 2, indicating their potential as a catalyst during the reaction. They were, however, subject to deactivation as shown in Figs. 3 and 4 as are common Ni catalysts [13]. In this study, the surface characterization described in Section 3.2 revealed that sintering and oxidation are the main cause of the deactivation. Carbon deposition, which is another major cause of deactivation of common supported Ni catalysts, was hardly observed, though the reason is not clear yet. It is thus not necessary to consider the effect.

Because the decrease in the BET surface area was small below 973 K (Table 1), agglomeration of the Ni particles is considered to be fairly suppressed. The fact that the Ni phase was not detected at 873 K, but was detected above 973 K in the XRD (Fig. 5) may support the slow agglomeration of the Ni particles below 973 K. Compared with the fine Ni particles, the porous surface seems to be less resistant to reaction and/or heat. The columnar structure in the porous surface changed into particles as shown in Fig. 6. This surface change must contribute to a decrease in the BET surface area to some extent. Oxidation was also very limited below 973 K as shown in Fig. 7(a). Ni was oxidized to form NiO at 973 K, but the extent of oxidation was so small that was barely detectable by TEM. Thus, the fine Ni particles are considered to continue playing a significant role as a catalyst, leading to the good stability below 973 K.

In contrast, sintering of the Ni particles must occur severely above 1073 K. The sharp decrease in BET surface area (Table 1) is the evidence of this. Formation of a thick oxide layer (Figs. 7(c) and (d)) shows that oxidation proceeded severely. Oxidation of Ni must directly lower the catalytic activity. In addition, Al_2O_3 and the more complicated $NiAl_{10}O_{16}$ are formed to cover the Ni particles Fig. 7, which may lead to the rapid loss of stability above 1073 K.

Table 2
Summary of the surface structures of the powder before and after 10-h reaction

	Before reaction	After 10-h reaction			
		873 K	973 K	1073 K	1173 K
Metal elements	Ni	Ni	Ni	Ni	Ni
Oxides			NiO	$NiO + Al_2O_3$	$NiO + Al_2O_3 + NiAl_{10}O_{16}$

5. Conclusions

The catalytic stability of the pretreated Ni_3Al powder for methane steam reforming was investigated by isothermal tests at 873, 973, 1073 and 1173 K for 10 h. The results are summarized as follows:

(1) The catalytic stability was good at temperatures below 973 K, especially at 873 K, where almost no deactivation occurred after 10 h. However, it decreased rapidly with reaction time at high temperatures above 1073 K.
(2) Fine Ni particles, which were produced in the pretreatment and served as a catalyst, were confirmed to survive on the outer surface after the tests under all conditions.
(3) Sintering of the fine Ni particles and oxidation were suppressed below 973 K, leading to the good stability, although both became obvious above 1073 K, leading to the rapid deactivation.

Acknowledgement

One of the authors (Yan Ma) acknowledges the National Institute for Materials Science for the provision of a NIMS Graduate Research Assistantship.

References

[1] G.W. Crabtree, M.S. Dresselhaus, M.V. Buchanan, Phys. Today 57 (12) (2004) 39.
[2] J.N. Armor, Catal. Lett. 101 (2005) 131–135.
[3] N.M. Bodrov, L.O. Apel'baum, M.I. Temkin, Kinetika i Kataliz 5 (1964) 696–705.
[4] J. Xu, G.F. Froment, AIChE J. 35 (1989) 88–96.
[5] M.A. Soliman, A.M. Adris, A.S. Al-Ubaid, S.S.E.H. El-Nashaie, J. Chem. Tech. Biotechnol. 55 (1992) 131–138.
[6] J. Wei, E. Iglesia, J. Catal. 224 (2004) 370–383.
[7] Y. Matsumura, T. Nakamori, Appl. Catal. A 258 (2004) 107–114.
[8] S. Rakass, H. Oudghiri-Hassani, P. Rowntree, N. Abatzoglou, J. Power Sources 158 (2006) 485–496.
[9] C. Pistonesi, A. Juan, B. Irigoyen, N. Amadeo, Appl. Surf. Sci. 253 (2007) 4427–4437.
[10] J.R. Rostrup-Nielsen, in: J.R. Anderson, M. Boudart (Eds.), Catalysis, Science and Technology, vol. 5, Springer-Verlag, Berlin, 1984, Chapter 1.
[11] J.R. Rostrup-Nielsen, J. Sehested, J.K. Nørskov, Adv. Catal. 47 (2002) 65–139.
[12] H.S. Bengaard, J.K. Nørskov, J. Sehested, B.S. Clausenb, L.P. Nielsen, A.M. Molenbroek, J.R. Rostrup-Nielsen, J. Catal. 209 (2002) 365–384.
[13] J. Sehested, Catal. Today 111 (2006) 103–110.
[14] C.T. Liu, D.P. Pope, in: J.H. Westbrook, R.L. Fleischer (Eds.), Intermetallic Compounds – Practice, vol. 2, John Wiley & Sons, Chichester, 1995, pp. 17–51.
[15] D.B. Miracle, R. Darolia, in: J.H. Westbrook, R.L. Fleischer (Eds.), Intermetallic Compounds – Practice, vol. 2, John Wiley & Sons, Chichester, 1995, pp. 53–72.
[16] Y. Xu, S. Kameoka, K. Kishida, M. Demura, A. Tsai, T. Hirano, Mater. Trans. 45 (2004) 3177–3179.
[17] Y. Xu, S. Kameoka, M. Demura, A. Tsai, T. Hirano, Intermetallics 13 (2005) 151–155.
[18] D.H. Chun, Y. Xu, M. Demura, K. Kishida, M.H. Oh, T. Hirano, D.M. Wee, Catal. Lett. 106 (2006) 71–75.
[19] D.H. Chun, Y. Xu, M. Demura, K. Kishida, M.H. Oh, T. Hirano, D.M. Wee, J. Catal. 243 (2006) 99–107.
[20] Y. Ma, Y. Xu, D.H. Chun, M. Demura, T. Hirano, Catal. Lett. 112 (2006) 31–36.
[21] J.T. Richardson, B. Turk, M.V. Twigg, Appl. Catal. A 148 (1996) 97.
[22] C. Wang, G. Gau, S. Gau, C. Tang, J. Bi, Catal. Lett. 101 (2005) 241–247.
[23] D. Świerczyński, S. Libs, C. Courson, A. Kiennemann, Appl. Catal. B: Environ. 74 (2007) 211–222.